EUROfusion

EUROFUSION CP(15)06/14

C. Gleason Gonzalez et al.

Simulation of Collisional Effects on Divertor Pumping in JT-60SA

12th International Symposium on Fusion Nuclear Technology (ISFNT)
Jeju Island, Korea
(14th September 2015 – 18th September 2015)

This work has been carried out within the framework of the EUROfusion Consortium and has received funding from the Euratom research and training programme 2014-2018 under grant agreement No 633053. The views and opinions expressed herein do not necessarily reflect those of the European Commission.

Simulation of Collisional Effects on Divertor Pumping in JT-60SA

C. Gleason-González[a*], S. Varoutis[a], X. Luo[a], K. Shimizu[b], T. Nakano[b], K. Hoshino[b], H. Kawashima[b], N. Asakura[b], Chr. Day[a], S. Sakurai[b]

[a]*Karlsruhe Institute of Technology, Hermann-von-Helmholtz-Platz 1, 76344, Germany*
[b]*Japan Atomic Energy Agency, 801-1, Mukoyama, Naka, Ibaraki 311-0193, Japan*

**Corresponding author : cristian.gleason@kit.edu*

In this work, the exhausted neutral gas flow is modeled for two cases of a simplified sub-divertor geometry and compared via three different approaches, namely (i) a collisionless approach based on the ProVac3D code, (ii) the DSMC approach based on the DIVGAS code that can be run with and without consideration of particle collisions, and (iii) the NEUT2D approach which has been extensively used in the past for the JT-60 design. In a first case study, the transmission probability was calculated by the 3 approaches and very good agreement is found between NEUT2D-ProVac3D whereas discrepancies between DIVGAS and NEUT2D are further analyzed. In the second case, the assessment of collisions is done by means of DIVGAS. It is found that the flow field is in the transitional regime with Kn numbers between 0.1 and 0.5. The DIVGAS collisionless case yielded lower values of temperature than the collisional one by factors of 0.5-0.8 in regions near the inlets of the sub-divertor whereas in regions near the pump and the chevron, the temperature difference is marginal. Moreover, a relative percentage difference of 20-70% in pressure values was found between collisionless and collisional approaches.

Keywords: Tokamak particle exhaust, Sub-divertor gas dynamics, Divertor pumping, DSMC, Vacuum

1. Introduction

Divertor pumping plays a key role in tokamak operation. In JT-60U, the modelling of particle exhaust was based on a collisionless approach [1], however for the foreseen high-density scenarios in JT-60SA [2,3] the use of more sophisticated models that can treat the transport of mass, momentum and energy by including neutral-neutral interactions is highly desirable. Based on this, the impact of intermolecular collisions can be assessed and further insights on the neutral particle dynamics of the exhaust process can be addressed. We intend here to carry out a major step in this direction by comparing collisionless and collisional solvers and addressing similarities and differences.

In this work for two example cases in a simplified geometry of the JT-60SA sub-divertor, the modelling of neutral flow is carried out and compared via three different approaches and codes: (i) ProVac3D [4] which exploits the characteristics of a Monte Carlo approach and, in the version used, does not consider collisions between the particles, (ii) DIVGAS [5], which is based on the Direct Simulation Monte Carlo method (DSMC) [6] and that can be run with and without consideration of collisions, and (iii) NEUT2D which is a collisionless approach that has been extensively used for JT-60U [7]. The NEUT2D code is coupled to the 2D plasma suite SONIC [1,8,9] whereas for the Monte Carlo approaches, the presence of the neutrals coming from the private region and divertor targets towards the sub-divertor has to be introduced by a proper choice of boundary conditions. On the other hand, for the DSMC method - and that is the core of the recently developed DIVGAS code (DIVertor GAs Simulator) – it has been successfully demonstrated that an accurate description of the typical sub-divertor conditions can be done under a wide range of collisionality regimes and in presence of high-temperature gradients taking into account complex geometries. Just recently, sub-divertor helium flow calculations for ITER were performed by implementing DSMC using SOLPS data [10] and a neutral gas dynamics study in the JET sub-divertor benchmarking DSMC against experimental data has been performed [5].

2. JT-60SA divertor pumping system

2.1 JT-60SA sub-divertor

In JT-60SA the W-shaped pumped divertor will exhaust the particles from the main chamber towards the cryopump location via two slots at the inner and outer divertor that re-direct the flow to the sub-divertor region (see arrows in Fig. 1) [11].

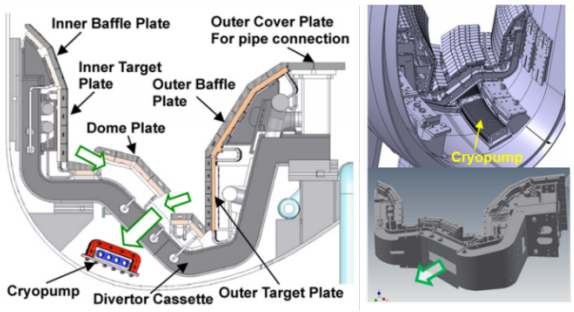

Fig. 1. The JT-60SA divertor geometry and pumping system.

For modelling purposes, the simplified 2D representation of the JT-60SA sub-divertor as routinely employed in SONIC calculations has been adopted as flow domain for all calculations, see Fig. 2. The inner (Gate 2) and outer (Gate 1) pumping slots act as open

author's email: cristian.gleason@kit.edu

boundaries where particle influx and outflux takes place. The pump surface absorbs particles with a well-defined capture coefficient. A chevron is placed at the entrance of the pumping duct and it acts as an obstacle for the gas flow, reducing the net throughput towards the cryopump.

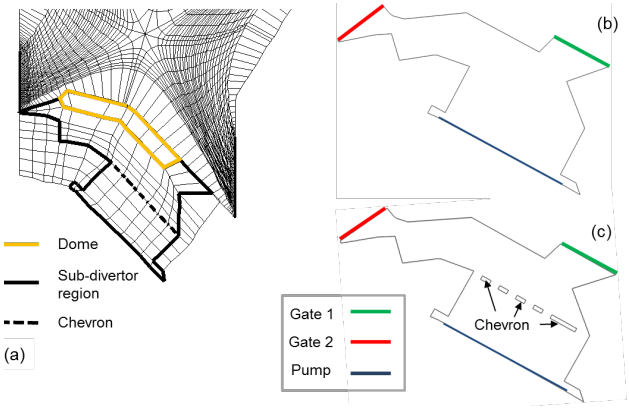

Fig. 2 (a) SONIC mesh including plasma main chamber, divertor dome ~~(yellow)~~ and sub-divertor region (bold) within the chevron shielding (dash). Sub-divertor domain (b) without and (c) with chevron employed in TPMC and DIVGAS calculations.

3. Modelling

3.1 NEUT2D and ProVac3D simulations

Both NEUT2D and ProVac3D model the neutrals without considering intermolecular interactions. Although a variety of atomic and molecular processes with plasma particles are treated in NEUT2D, in this work a simplistic version of its physics is employed, as described later in Section 3.3. ProVac3D is different from the classical ray trace test particle Monte Carlo approach in the sense that particle velocities are being involved. The basic hypothesis is that the density in one cell of the model is proportional to the accumulation of time of flight of every molecule in this cell and inversely proportional to the cell volume. The advantage over the conventional approach is that this also holds if the system has strong directional flow at non-equilibrium state. ProVac3D has been successfully applied to ITER NBI [12].

3.2 DIVGAS simulations

The collisional DIVGAS code is based on the DSMC method which is a particle-based, numerical scheme for solving the non-linear Boltzmann equation [6]. In the DSMC approach, each model particle represents an effective number of real atoms (and/or molecules) in the physical system. The model particles are sorted into cells and the particles' time evolution is done in time steps of duration Δt in which their free motion and collisions between them are uncoupled. The present DIVGAS calculations were implemented within the framework of an open-source C++ toolbox for computational fluid dynamics: OpenFOAM [13], where the DSMC solver, *dsmcFoam*, has been rigorously validated for a variety of benchmark cases [14, 15] and was modified accordingly for the purpose of the present work. For completeness and clarity, specific matters of the implementation are provided in the following section.

A rectangular grid with a total number of cells of 1.5×10^3 was employed. In order to achieve less statistical scattering and to increase the accuracy of the numerical results, in all calculations the average number of 100-400 particles per cell was chosen. The number of collisions per cell is calculated using the No Time Counter scheme and the intermolecular potential between particles is short-ranged and follows the Larsen-Borgnakke variable hard sphere model. In our calculations, the time increment was taken as $\Delta t = 1\ \mu s$. We found, that this value, which is a fraction of the mean collision time of the particle, ensures that the decoupling between free motion and collisions holds.

3.3 Study cases: simplified pumping setup and modified JT-60SA Scenario #2

The comparison between the neutral solvers is done in the framework of two different divertor pumping setups. For the first setup, the *simplified case*, the solvers are cross-checked in terms of the reproduction of the transmission probability. This characteristic is defined as the ratio of particles which reach an outlet once they have been released at an inlet. For this case, particle influx (D_2) with a Maxwellian velocity distribution and at an average temperature of T = 293.16 K is generated at only Gate 2 and the outflux at Gate 1 and the pump position is calculated. Both gates are seen as open surfaces with a sticking coefficient of 100%, i.e. particles coming from the sub-divertor and impinging these surfaces are absorbed instantly. No chevron is considered in this simplified case and the capture coefficient at the pumping surface is set to 3% of the total incoming flux. The rest, 97% is reflected back to the sub-divertor domain with a cosine distribution at a temperature of 293.16 K. Similarly, the D_2 molecules are diffusely reflected from the sub-divertor walls at a temperature of T_w = 293.16 K.

The second setup is based on the JT-60SA Scenario #2 [11], where the particle handling needs to be fulfilled at full injection power of 41 MW for pulses of 100 s (high-particle loads). A dedicated SONIC calculation was performed for this, where the atomic deuterium influx at the gates is not considered at this stage (we therefore call it *modified scenario #2*). The boundary conditions taken from the SONIC run to be applied in DIVGAS read as follows: the deuterium molecule influx to the sub-divertor was found at particle rates of 1.26×10^{23} 1/s (Gate 1) and 5.016×10^{23} 1/s (Gate 2). The particles have a flow speed of 314.3 m/s (Gate 1) and 589 m/s (Gate 2). The translational temperatures of the particles at Gate 1 and 2 are 1118.57 K and 1335.67 K, respectively while the temperature of the sub-divertor walls is set to 293.16 K. The pure diffuse reflection model is used as before. At the pumping surface, the employed capture coefficient and reflection coefficients are the same as in the *simplified* case. A chevron in front of the pumping duct is now included. As mentioned before, the objective of the present work is to isolate the effect of the collisions on the sub-divertor flow, which is

accomplished in the framework of this paper on single gas flow level. If needed for future optimization studies, it is of course straight forward to introduce more species. Furthermore, at this stage, any toroidal effects in the flow are neglected.

4. Results and discussion

4.1 Simplified setup: Transmission probability

The first cross-check between collisionless solvers is summarized in Table 1 where the outflux is normalized to the influx at Gate 2. The versatility of DIVGAS to not consider the intermolecular interactions by *turning off* the collision module in the code has been used. By doing this, a direct comparison of the transmission probability between codes can be performed. More than $2\text{x}10^6$ model particles were used in the present DIVGAS modelling. Regarding ProVac3D calculations, 10^{12} test particles were employed in order to estimate the transmission probability of the system. This difference is one reason to explain the larger deviation between the purely collisionless codes and the DIVGAS with switched off collision kernel.

Table 1. Transmission probability for the collisionless case: NEUT2D, ProVac3D and DIVGAS.

	Normalized outflux		
	NEUT2D	ProVac3D	DIVGAS
Gate 1	0.143464	0.143626	0.162628
Gate 2	0.841573	0.841844	0.813512
Pump	0.014963	0.014829	0.023859

The capture coefficient of 3% towards the pump side is fulfilled in ProVac3D simulations by monitoring the ratio of the absorbed particles to the total number of hits, yielding a value whose relative difference is $1.8\text{x}10^{-5}$ with respect to the defined value of 0.03. In DIVGAS, the final monitoring of the absorbed particles relative to the incoming flux towards the pump surface yields a value of 3.03%. This is in line with the numbers shown in the Table 1 above (transmission probabilities to Gate 1 and Pump higher in DIVGAS than in NEUT2D, ratio at Gate 2 itself lower) and due to the fact that, following the total mass conservation in the system, a reduction of outflux at Gate 2 translates in a natural increase of the outflux at both Gate 1 and pump.

In this collisionless framework, further analysis is carried out by comparing the macroscopic variables stored at each cell in the sub-divertor domain in both NEUT2D and DIVGAS as follows: the sub-divertor was further divided in 4 different sub-domains as shown in Fig. 3 and both code outputs where compared at the nodes where the NEUT2D cell values are defined (shown inside the boxes).

The DIVGAS velocity profiles sampled at different locations in regions I-IV (see Fig. 4) are in good agreement with the corresponding NEUT2D calculations. For instance, by analyzing the profiles from top of region IV to end of it (up to the pump surface, i.e. increasing the l-index) it was found that the profiles show qualitatively the same functional dependence in real-space coordinates. As the profile moves towards the pump, the magnitude of the velocity decreases considerably in both codes (factor of 10). This can be explained by the fact that the particles being reflected by the pump (97% of incident flux) have a thermal speed of ~ 1x103 m/s that counteracts the total incident flux, resulting in a reduced net velocity (the contributions in all directions of individual particles define the velocity at each cell).

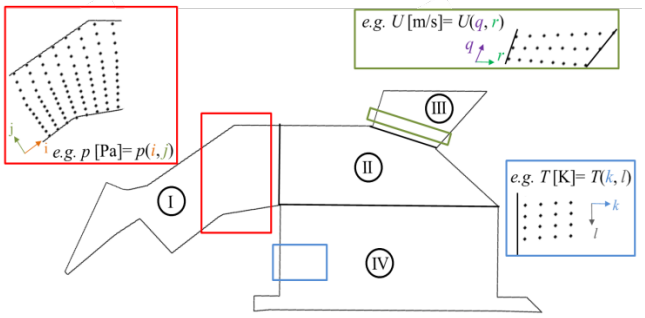

Fig. 3. JT-60SA sub-divertor is divided in 4 regions (I-IV). DIVGAS and NEUT2D values of U, p, T and n are compared at the same node location. At each node, with a corresponding point (x, y) in real-space, a pair of indexes is associated to it in order to ease the comparison in the regions.

Despite the good agreement in velocity profiles, the values of number density and temperature of NEUT2D across the computational domain are a factor of 0.6-0.8 and 0.15-0.5 below DIVGAS values, respectively. Regarding the temperature, DIVGAS considers the rotational and translational modes in order to calculate the total temperature in each cell of the computational domain. This results for instance in region III, in a difference of 15% between T_{DIVGAS} and T_{NEUT2D}. By comparing only the translational contribution of temperature, the agreement between codes ameliorates by 5% regarding the temperature values. The expected agreement between codes near the pumping surface (Fig. 4 bottom-right, l=9, k) is found since particles are being desorbed with same temperature. The percentage difference in T is found to be less than 2% between both codes. However, at this location a ratio of n_{NEUT2D}/n_{DIVGAS} ~ 0.7 is found. This might be one more reason for the discrepancies found in the outflux values in Table 1. Regarding region II, it is found that the velocity profiles have a relative difference of 5-10% between DIVGAS and NEUT2D, whereas the density calculated by NEUT2D is always below DIVGAS values by a factor of 0.7-0.8. The temperature distribution in this region differs notably. For instance, a region of high-temperature in DIVGAS (border of region I and II) due to high-translational kinetic energy contribution of gas coming from Gate 2 is a *cold* region in NEUT2D (compared to the rest of NEUT2D values in region II), where it is found that T_{DIVGAS}/T_{NEUT2D} ~ 1.5. Furthermore, the expansion into vacuum at Gate 1 (open boundary) is seen in DIVGAS by noticing the decrease in temperature near the border of region II and III.

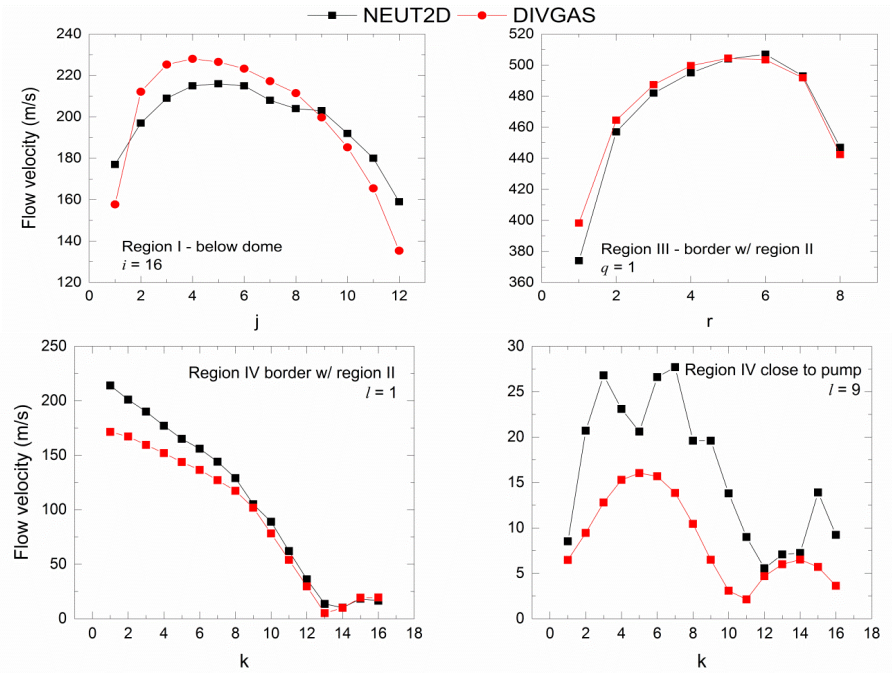

Fig. 4. Top: Velocity profiles along specific nodes of region I (below the dome) and III (close to Gate 1). Bottom: Velocity profiles sampled across the duct towards the pump. The positions of the pairs (i,j), (q,r) and (k,l) in the sub-divertor are referred in Fig. 3.

4.2 Scenario #2: collisional effects

As a pre-requisite to properly compare with the values of pressure, temperature, density and flow velocity as obtained from NEUT2D, the corresponding influx and outflux conditions in the sub-divertor, which result from the plasma to neutral coupling within SONIC, have to be nicely matched. The fluxes in the SONIC suite calculations at the gates are typically asymmetric, translating into a non-Maxwellian velocity distribution. Therefore, by using the present version of DIVGAS, the challenging task is to match the non-symmetric boundary conditions at the gates with the restriction that the particle influx, based on the DSMC algorithm, is derived from a Maxwellian distribution. Simulations, see some results plotted in Fig. 5, showed that in order to match the macroscopic variables at Gate 2, it is necessary to increase the angle of influx velocity with respect to the normal of the surface, yielding an optimum angle of 85.81° (needed for a p_{NEUT2D} = 4.44 Pa at Gate 2) whereas an angle of 0° is sufficient at Gate 1. At Gate 2, the smaller the angle between the flow velocity and the surface normal, the higher value of particle impinging the sub-divertor wall is seen and thus, most of the gas is then diffusely reflected towards Gate 2 deviating even more from the reference NEUT2D pressure value.

On the other hand, the modelling approach of the capture coefficient at the pump was done by monitoring the amount of particles impinging the pumping surface and the net particle rate occurring just above the pumping surface. The chevron structure is now considered in the calculations, as shown in Fig. 2c, the length of its structures are placed in such a way that it is intended to block half of the total particles entering the duct.

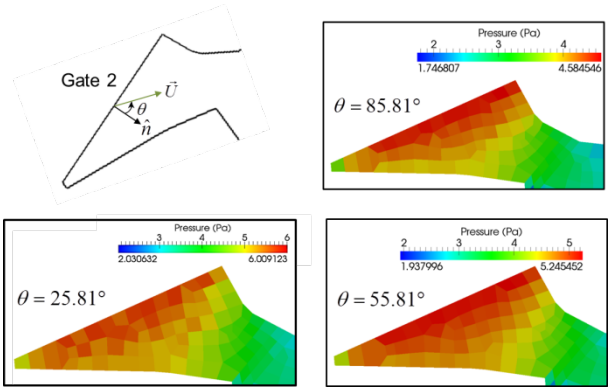

Fig. 5. Variation of incidence angle of flow velocity in Gate 2 respect to its surface´s normal vector.

By means of DIVGAS, the assessment of collisional effects is performed by *switching* on the collision module in the code. Here, pressure, temperature and *Kn* number were subjects of study. Simulations shown that whenever the collisions are taken into account the pressure in the sub-divertor is increased by 20-60% in regions far from the Gates, namely in region I (below the dome) and II. In region IV, the discrepancy between the collisionless and collisional case is increased furthermore and a 70% difference is found. Fig. 6 illustrates the contour plot and isobars along the JT-60SA sub-divertor for both cases.

The effect of collisions can also be seen in the temperature distribution of the flow. An interesting aspect is the temperature peak near Gate 2 and 1. For the collisionless case, the overall temperature in the sub-

divertor is at least a factor of 0.5 lower than the collisional one near both gates whereas in region II the ratio of temperatures is close to 1, as shown in Fig. 7.

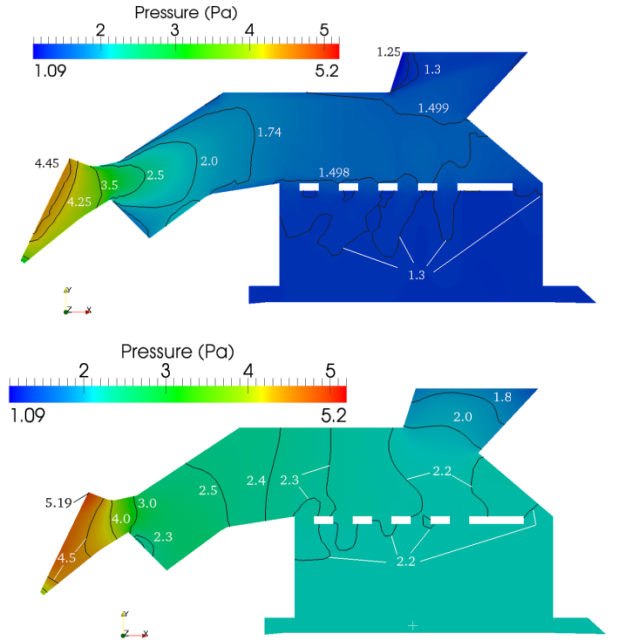

Fig. 6. Top: Isobars in DIVGAS simulations (collisions off). Bottom: Isobars in DIVGAS (collisions on).

.

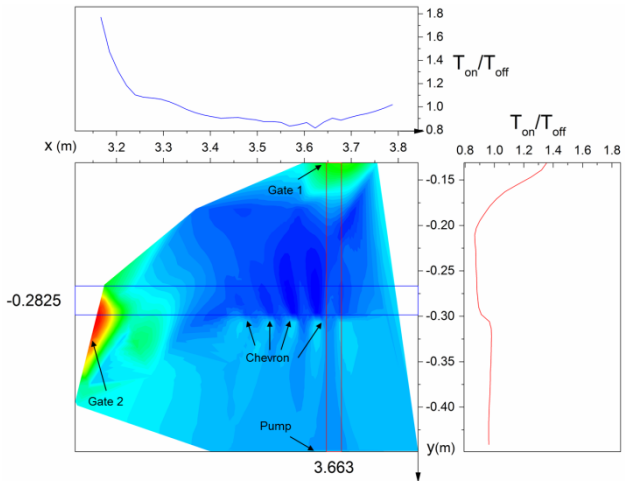

Fig. 7. DIVGAS temperature ratio of collisions-on case to collisions-off case denoted by T_{on}/T_{off} along the sub-divertor. A plot of the variation of the ratio over a selected vertical (right) and horizontal lines (top) is also shown.

The gas undergoes an expansion from a high-pressure region into a lower-pressure region and thus a change in the flow velocity is seen (hence the temperature, $T \sim \langle v^2 \rangle_{mol} - U^2$). This effect becomes stronger with increasing collisionality, since the temperature is a direct manifestation of intermolecular interaction. The collisionality regime can be determined via the *Kn* number, defined as the ratio of the mean free path to the characteristic length of the sub-divertor. The latter is chosen to be the narrowest distance between the dome sub-divertor wall in region I (0.045 m). Fig. 8 is illustrating the sub-divertor collisionality in terms of the calculated *Kn* number. Such a plot can only be done with a code that considers collisions (in the collision-free case there results a *Kn* number of infinity).

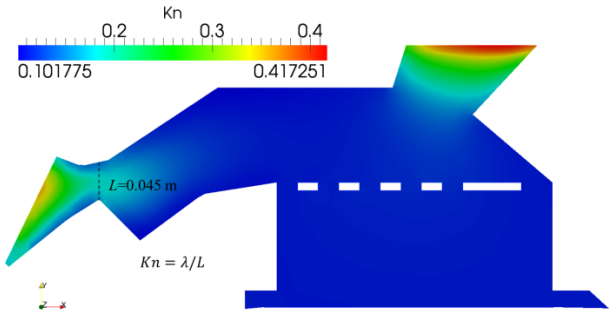

Fig. 8. The Kn number profile along the JT-60SA sub-divertor.

It is known that the influence of collisions can be neglected only in the region *Kn*>10, whereas in our case we find the *Kn* number to be below 0.5 in the whole sub-divertor area. This implies the transitional flow regime which is defined for *Kn* values between 0.1 up to 10 [16], where neither a free collisional nor a continuum approach are sufficient to describe the flow dynamics. This justifies strongly the necessity to consider collisions if one needs to have a physically correct description of the flowfield in this area. It is to be noted, however, that the inclusion of atomic deuterium in the calculations should be done in a future step to validate this conclusion, particularly because the high-energetic atoms coming from the private flux region and being reflected rom the targets will enhance the momentum exchange at the gates and this effect needs to be quantified.

5. Summary

The sub-divertor gas flow in JT-60SA is simulated for 2 example cases, namely a simplified setup with only one source term (namely Gate 2) and a second setup which is related to JT-60SA Scenario #2.

The scenario with a simplified setup is simulated using two intrinsic collisionless approaches: ProVac3D and NEUT2D and a third approach: DIVGAS, which has been used without its collision module for a direct comparison with the other two. The transmission probability was estimated by all the approaches, yielding a very good agreement between NEUT2D and ProVac3D whereas discrepancies where found between DIVGAS and NEUT2D calculations. This was further explored by comparing the densities, temperatures and flow velocity in the sub-divertor. It was found that the flow velocities have an excellent agreement, but the densities and temperatures calculated by NEUT2D are lower by factors in the range of 0.6-0.7 and 0.15-0.5, respectively.

In modelling the modified Scenario # 2, the assessment of collisionality was done. The gas flow is simulated by using DIVGAS with and without collisions. Collisions were found to have a significant impact on the macroscopic variables along the sub-divertor. The discrepancies between DIVGAS collisional and collisionless in temperature values are present and

simulations show that the collisionless case has lower values of temperature than the collisional case by a factors in the range of 0.5-0.8 in regions I and III, whereas in region II and IV the temperature difference is marginal. Moreover, a relative percentage difference of 20-70% in pressure values was found between collisionless and collisional approaches. The calculation of the Knudsen number was performed in order to have an idea of the collisionallity flow regime in the sub-divertor. Values between 0.1-0.41 suggest that the sub-divertor gas flow is in the transitional regime, where neither a pure free molecular nor a continuum approach is sufficiently accurate to describe the dynamics of the flow. This work presents the capabilities and advantages of using collisional solvers in tackling moderate- and high-density sub-divertor flows.

Acknowledgments

This work has been carried out within the framework of the EUROfusion Consortium and has received funding from the EURATOM research and training programme 2014-2018 under grant agreement No 633053. The views and opinions expressed herein do not necessarily reflect those of the European Commission. Part of the simulations presented herein were carried out at the computational resource bwUniCluster funded by the Ministry of Science, Research and Arts and the Universities of the State of Baden-Württemberg, Germany, within the framework program bwHPC; and part were carried out using the HELIOS supercomputer system at Computational Simulation Centre of International Fusion Energy Research Centre (IFERC-CSC), Aomori, Japan, under the Broader Approach collaboration between Euratom and Japan, implemented by Fusion for Energy and JAEA.

References

[1] H. Kawashima et al., J. Nucl. Mater. 363–365 (2007) 786–790.

[2] J. Garcia et al., Nucl. Fusion 54 (2014) 093010.

[3] JT-60SA Research Unit, JT-60SA Research Plan, Feb. 2015, http://www.jt60sa.org/.

[4] X. Luo, Chr. Day, Investigation of a new Monte Carlo method for the transitional gas flow, Proc. of the 27th Int. Symposium on Rarefied Gas Dynamics, AIP Conf. Proceedings 1333 (2011) 272-276.

[5] S. Varoutis et al., Simulation of neutral gas flow in the JET subdivertor and comparison with experimental results, Proc. 25th IAEA Fusion Energy Conf. St. Petersburg, Russia, Oct. 2014, submitted to Nuclear Fusion.

[6] G. A. Bird, Molecular Gas Dynamics and the Direct Simulation of Gas Flows, 2nd ed. Oxford: Oxford University Press, 1994.

[7] K. Shimizu et al., Simulation of divertor detachment characteristics in JT-60 with superconducting coils, J. Nucl. Mater. 313–316 (2003), SUPPL.1277–1281.

[8] H. Kawashima et al., Nucl. Fusion 49 (2009) 065007.

[9] H. Kawashima, et al., Plasma Fusion Res. 1 (2006) 031.

[10] C. Gleason-González, S. Varoutis, V. Hauer, and C. Day, Fusion Eng. Des. 89 (2014) 1042–1047.

[11] Y. Kamada, et al., Nucl. Fusion 51 (2011) 073011.

[12] X. Luo and C. Day, Fusion Eng. Des. 85 (2010) 1446–1450.

[13] "OpenFOAM Foundation," 2015. [Online]. Available: http://www.openfoam.org/.

[14] T. J. Scanlon et al., Thermochemistry Modelling in an Open Space DSMC Code, 28th Int. Symp. Shock Waves, pp. 1–7, 2011.

[15] C. White, M. K. Borg, T. J. Scanlon, and J. M. Reese, Comput. Fluids 71 (2013) 261–271.

[16] M. Gad-el-Hak and W. Seemann, "MEMS Handbook," Applied Mechanics Reviews, vol. 55, no. 6. p. B109, 2002.